



Contents lists available at ScienceDirect

Journal of Non-Crystalline Solids

journal homepage: www.elsevier.com/locate/jnoncrysol

Preparation and characterization of ZnO particles embedded in organic–inorganic planar waveguide by sol–gel route

A. Chiappini^{a,*}, C. Armellini^a, A. Chiasera^a, M. Ferrari^a, R. Guider^b, Y. Jestin^a, L. Minati^c, E. Moser^d, G. Nunzi Conti^e, S. Pelli^e, R. Retoux^f, G.C. Righini^{e,g}, G. Speranza^c^a CNR-IFN, Istituto di Fotonica e Nanotecnologie, CSMFO Lab., via alla Cascata 56/c, I-38050 Povo-Trento, Italy^b Laboratorio Nanoscienze, Dipartimento di Fisica, Università di Trento, via Sommarive 14, I-38050 Povo-Trento, Italy^c Physics and Chemistry of Surfaces and Interfaces, FBK-IRST, Sommarive Str. 18, I-38050 Povo-Trento, Italy^d Dipartimento di Fisica, CSMFO Group, Università di Trento, via Sommarive 14, I-38050 Povo-Trento, Italy^e MDF Lab., Nello Carrara Institute of Applied Physics, IFAC – CNR, via Madonna del Piano 10, I-50019 Sesto Fiorentino, Italy^f Laboratoire CRISMAT, UMR 6508, ENSICAEN, 6 Bld. Maréchal Juin, 14050 Caen cedex, France^g CNR, Department of Materials and Devices, via dei Taurini 19, 00185 Roma, Italy

ARTICLE INFO

Article history:

Available online 11 May 2009

PACS:

32.30.Jc
33.20.Rm
42.82.Fv
71.20.Rv
81.07.Pr
81.20.Fw
84.40.Az

Keyword:

Planar waveguides

ABSTRACT

Hybrid organic–inorganic waveguides based on ZnO-(3-glycidoxypropyl)trimethoxysilane (GPTS) have been fabricated by sol–gel route. A transparent sol of ZnO was added to the GPTS host and the resulting sol was deposited on silica substrates by spin coating technique. Waveguides with different molar composition $(100-x)\text{GPTS}-x\text{ZnO}$ ($x = 10, 20, 30$) were investigated by different diagnostic techniques. Morphological measurements were carried out by means of an AFM apparatus, and a roughness of few nanometers was estimated for all the waveguides. Optical properties such as refractive index, thickness, number of propagating modes and attenuation coefficient were measured at 632.8, 543.5, 1319 and 1542 nm by the prism coupling technique as a function of the ZnO content. Photoluminescence measurements, upon excitation at 325 nm, showed a large luminescence band in the region between 350 and 600 nm with a main peak centered at about 380 nm, due to the presence of ZnO nanoparticles.

© 2009 Elsevier B.V. All rights reserved.

1. Introduction

More and more, optical processing needs many functions to be assembled. Planar lightwave circuits are generally expected to give a solution for integrated optical functions [1].

For this purpose, both low cost technology and high density scale integration are required.

One possible fabrication process to satisfy this demand is the sol–gel route. It is considered as a versatile, flexible and a low-cost technique useful for the realization of integrated photonic devices. [2,3]. In particular, the technologies based on organic materials offer a great deal of potential for performing integrated circuits [4–6]. One of the organic materials largely employed in several different applications, such as antiscratch coatings [7], contact lens materials [8], passivation layers for microelectronics [9], and

multifunctional coatings [10] is the (3-glycidoxypropyl)trimethoxysilane (GPTS).

Recently, it was shown that using GPTS matrix it is possible to obtain passive optical planar waveguides [11–13] as well as hybrid thin films of TiO_2/GPTS activated by erbium oxide nanocrystals [14].

On this scenery the develop of new materials based on GPTS organic matrix can be considered extremely interesting in the field of integrated optics opening the possibility to realize active planar waveguides incorporating into the matrix active organic molecules or semiconductor nanoparticles. As far as concerns the latter possibility there is a great effort in realizing novel systems suitable for exploiting the particular properties of ZnO. For instance, it is well known that ZnO is extremely efficient as piezoelectric materials and it is a promising material for short-wavelength optoelectronic devices [15,16].

In this paper, we report the procedure used to realize low losses hybrid-organic–inorganic waveguides constituted by GPTS–ZnO, with a tailored refractive index depending on the organic/inorganic molar ratio. Optical, structural and spectroscopic properties of the waveguides are investigated.

* Corresponding author. Tel.: +39 0461881695; fax: +39 0461881696.

E-mail address: chiappini@science.unitn.it (A. Chiappini).URL: <http://www.science.unitn.it/~gcsmf/> (A. Chiappini).

2. Experimental

Three different waveguides, with the following molar ratio GPTS:ZnO = 90:10, 80:20 and 70:30, hereafter labeled *W*(90:10), *W*(80:20) and *W*(70:30), were realized using the protocol below reported.

First of all the sol used for the deposition of the organic–inorganic matrix was prepared in two steps:

- (i) the polymeric part was realized starting from GPTS, which was diluted in butanol (volume ratio 1:0.5).

Moreover, a prehydrolysis treatment was performed by addition of HCl 0.1 M. The molar ratio GPTS:H₂O was 1:0.5.

The resulting solution was submitted to vigorous stirring overnight at room temperature before adding the inorganic sol.

- (ii) For the ZnO precursor part, zinc acetate was used as the starting reagent. The acetate was dissolved in 2-propanol with a molar ratio of 1:5. For total dissolution of the acetate 0.006 mol diethanolamine was added to the sol. After stirring for 2 h a transparent sol was obtained.

The above two solutions were mixed and stirred for another 2–3 h to obtain the desired sol for deposition.

Thin films were deposited on square SiO₂ substrates by spin coating using the following speed parameters:

- Step1: speed 800 rpm for 50 s; acceleration 133 rpm;
Step2: speed 2000 rpm for 1 s; acceleration 133 rpm;
Step3: speed 800 rpm for 50 s; deceleration 133 rpm.

Subsequently the films were treated by ultraviolet (UV) exposition with a UV lamp emitting at 360 nm and then heated at 150 °C for 1 h in order to achieve densification.

The refractive index and the thickness of the waveguides were measured for both transverse electric (TE) and transverse magnetic (TM) polarization by an *m*-line apparatus (Metricon mod. 2010) based on the prism coupling.

In order to measure propagation losses the light intensity scattered out of the waveguide plane, which is proportional to the guided intensity, was recorded by a fiber probe scanning down the length of the propagating streak. The losses were evaluated by fitting the intensity to an exponential decay function, assuming a homogeneous distribution of the scattering centers in the waveguides [13].

The morphology of the waveguides was investigated using an AFM NT-MDT P47H apparatus, in order to determine the roughness of the surface of the samples.

Photoluminescence (PL) emission spectra were recorded at room temperature with a Varian Eclipse fluorescence spectrophotometer equipped with xenon lamp as excitation source.

3. Results

Table 1 reports the optical parameters of the organic–inorganic waveguides with different molar content of ZnO and GPTS obtained by modal measurements.

Fig. 1 reports the refractive index profile of the waveguide *W*(80:20) and Fig. 2 shows the squared electric field profile of the TE₀ mode for the waveguide *W*(90:10) calculated at 1542 nm (Fig. 2(a)) and at 632.8 nm (Fig. 2(b)) by using the parameters obtained by the *m*-line measurements.

Fig. 3 shows a AFM image of the planar waveguide *W*(80:20), where the average roughness measured using NT-MDT P47H apparatus, was about 3 nm, for all the waveguides.

Table 1

Optical parameters measured at 543.5, 632.8, 1319 and 1542 nm (TE polarization) for the ZnO–GPTS planar waveguides. Attenuation coefficient is measured by exciting the TE₀ mode.

Waveguides labeling (GPTS:ZnO)	<i>W</i> (90:10)	<i>W</i> (80:20)	<i>W</i> (70:30)
Number of modes at 632.8 nm	3	3	2
Number of modes at 543.5 nm	4	2	2
Number of modes at 1319 nm	2	1	1
Number of modes at 1542 nm	1	1	1
n_{film} at 543.5 nm	1.501 ± 0.005	1.510 ± 0.005	1.517 ± 0.005
n_{film} at 632.8 nm	1.497 ± 0.005	1.506 ± 0.005	1.513 ± 0.005
n_{film} at 1319 nm	1.487 ± 0.005	1.498 ± 0.008	1.501 ± 0.008
n_{film} at 1542 nm	1.485 ± 0.008	1.496 ± 0.008	1.499 ± 0.008
Film thickness (μm)	3.2 ± 0.1	2.2 ± 0.1	1.2 ± 0.1
Attenuation coefficient at 1542 nm (dB/cm)	0.4 ± 0.1	0.7 ± 0.1	1.5 ± 0.1

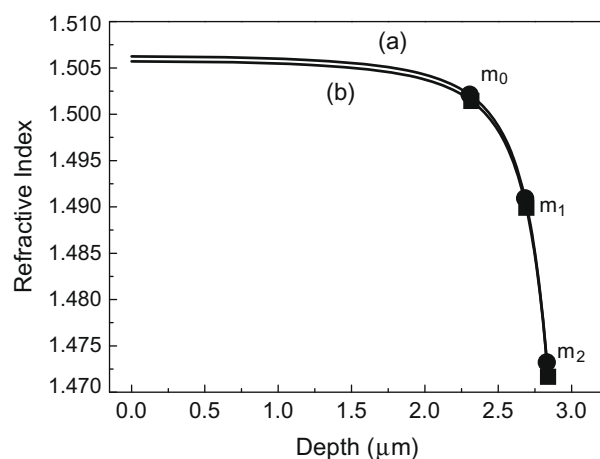


Fig. 1. Refractive index profiles of the organic–inorganic planar waveguides *W*(80:20) reconstructed from modal measurements at 632.8 nm for: (a) the TE and (b) TM polarization. The effective indices of the TE (●) and TM (■) modes are reported.

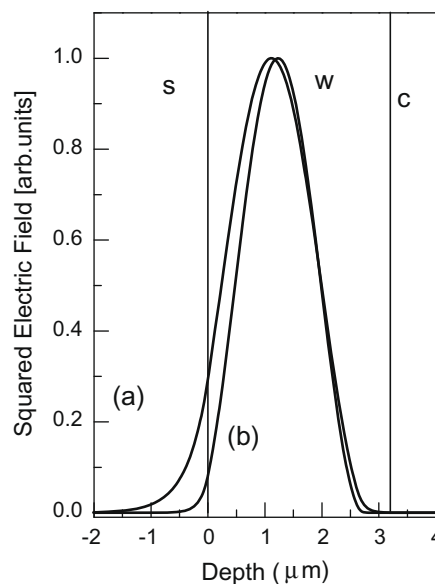


Fig. 2. Calculated squared electric field profiles of the TE₀ mode at 1542 (a) and 632.8 nm (b) across the layered structure, cladding of air C, waveguide W, and the SiO₂ substrate S of the *W*(90:10) planar waveguide.

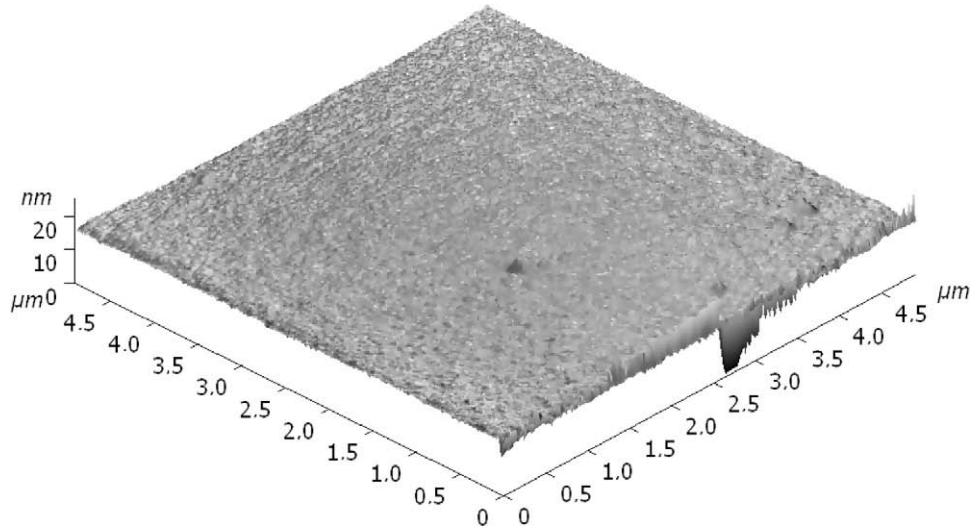


Fig. 3. AFM image of the top surface of the planar waveguide W(80:20). The average roughness was about 3 nm.

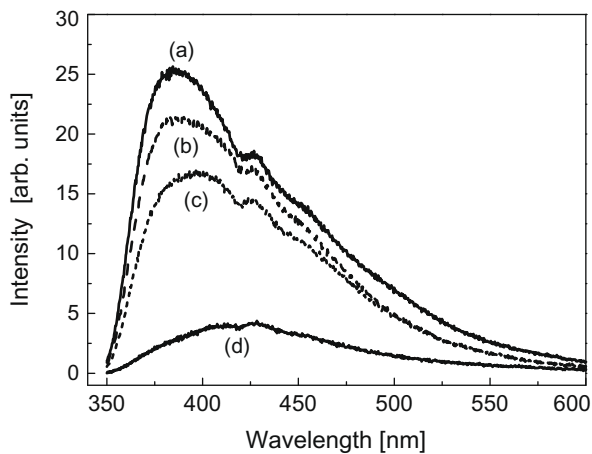


Fig. 4. Room temperature PL measurements of the waveguides: W(70:30) (a), W(80:20) (b), W(90:10) (c) and of the blank film (d) (GPTS without ZnO).

In Fig. 4 are reported the PL spectra of the waveguides W(70:30) (Fig. 4(a)), W(80:20) (Fig. 4(b)), W(90:10) (Fig. 4(c)), and of a blank sample (Fig. 4(d)) obtained upon excitation at $\lambda_{exc} = 325$ nm. The blank sample was obtained following the same protocol used to realize the waveguides but without adding to the final sol the inorganic content of zinc acetate.

4. Discussion

From Table 1, we can notice that the waveguides support many propagating modes depending on their thickness, refractive index, and exciting wavelength. As expected, the refractive index of the film increases with the nominal inorganic content. The observed variation is of the same order of magnitude of that observed in related organic–inorganic hosts containing HfO₂ nanoparticles [13] and in particular the GPTS–ZnO–W(90:10) planar waveguide exhibits an attenuation coefficient of 0.4 dB/cm, which is reasonably low for the wavelength of interest in the field of integrated optics. This value is comparable with those reported in others works [17–19].

The refractive index profile of the waveguides was reconstructed from the effective indices at 632.8 nm, by an inverse Wentzel–Kramers–Brillouin method [20].

From Fig. 1, we can observe that the waveguide exhibits a single step profile with a uniform refractive index throughout the thickness. The very small difference of the refractive index profiles obtained for TE and TM modes indicates that the birefringence in this waveguide is negligible. The other waveguides exhibit a similar behavior.

The modeling of the square electric field, reported in Fig. 2, indicates that the optical parameters of the waveguide, i.e. refractive index and thickness, appear appropriate for application in the third telecommunication window. In fact, the ratio of the integrated intensity, i.e. the square of the electric field in the waveguide to the total intensity, which includes also the squared evanescent field, is 0.99 and 0.94 at 632.8 nm and 1542 nm, respectively. This means that an efficient injection at 1542 nm is possible for the produced waveguide.

From AFM measurements, reported in Fig. 3, it is possible to observe that the realized waveguides are free-cracks and an average roughness of 3 nm is determined, for all the waveguides, confirming that the losses due to the surface roughness are negligible.

The spectra of Fig. 4 show that the films exhibit a very large luminescence band covering the range between 350 and 600 nm. Moreover, it is evident that the waveguides containing more inorganic part present a more intense PL in the region at about

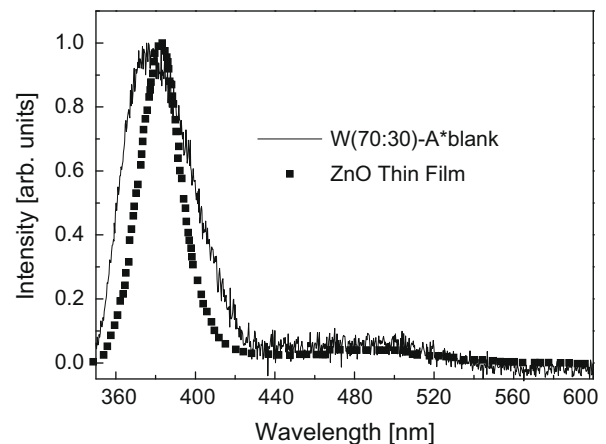


Fig. 5. The continuous line drawn spectrum is obtained by subtracting the spectrum of the blank film from that of W(70:30) waveguide. The dotted line corresponds to the PL spectrum of ZnO thin film reported in Ref. [21].

380 nm. Fig. 5 shows the procedure used in order to separate the contribution of ZnO from that of the matrix. The photoluminescence spectrum due to ZnO is estimated by subtracting from the spectrum of the W(70:30) waveguide the spectrum of the blank film multiplied by a factor A ($W(70:30) - A \times \text{blank}$). The resulting spectrum is compared to that of ZnO crystallized thin film as obtained from Ref. [21] (Fig. 5 dotted line). The shape of the calculated spectrum shows the classical shape of ZnO, where it is possible to distinguish a main emission in the UV region, due to the bound excitation emission [22,23] and one weaker emission in the visible region mainly due to the intrinsic defects such as zinc/oxygen interstitials, zinc/oxygen vacancies [24]. This procedure leads to the conclusion that the peak at about 380 nm can be attributed to the presence of ZnO nanoparticles.

5. Conclusions

Hybrid organic–inorganic waveguides of different molar content, based on ZnO-(3-glycidoxypropyl)trimethoxysilane (GPTS), were prepared by sol–gel technique.

AFM measurements put in evidence an average roughness of 3 nm for all the waveguides. Optical parameters indicate that the waveguides present a negligible birefringence, a significant confinement, and an attenuation coefficient equal 0.4 dB/cm for the W(90:10) waveguide. PL measurements showed a large luminescence band in the region between 350 and 600 nm; and a main peak centered at about 380 nm due to the presence of ZnO nanoparticles.

Acknowledgements

This research was performed in the framework of the Projects PAT-FaStFal 2007–2010 and COST MP0702: Towards Functional Sub-Wavelength Photonic Structures.

References

- [1] S. Toyoda, A. Kaneko, N. Ooba, M. Hikita, H. Yamada, T. Kurihara, K. Okamoto, S. Imamura, in: Proceedings ECOC'98, 1998, p. 103.
- [2] R.R. Gonçalves, G. Carturan, L. Zampedri, M. Ferrari, M. Montagna, A. Chiasera, G.C. Righini, S. Pelli, S.J.L. Ribeiro, Y. Messaddeq, Appl. Phys. Lett. 81 (2002) 28.
- [3] P. Grosso, I. Hardy, I. Assa, T. Batté, S. Haesaert, B. Vinouze, Opt. Commun. 235 (2004) 281.
- [4] R. Moosburger, R. Hauffe, U. Siebel, D. Arndt, J. Kropp, K. Petermann, IEEE Photon. Technol. Lett. 11 (1999) 848.
- [5] X.M. Du, Tahar Touam, L. Degachi, J.L. Guilbault, Mark P. Andrews, S. Iraj Najafi, Opt. Eng. 37 (1998) 1101.
- [6] I. Hardy, P. Grosso, D. Bosc, IEEE Photon. Technol. Lett. 17 (2005) 1028.
- [7] Haoying Li, Yunfa Chen, Chengxiang Ruan, Weimin Gao, J. Nanopart. Res. 3 (2001) 157.
- [8] G. Philipp, H. Schmidt, J. Non-Cryst. Solids 63 (1984) 283.
- [9] M. Popall, J. Kappel, M. Pilz, J. Schulz, G. Feyder, J. Sol–Gel Sci. Technol. 2 (1994) 157.
- [10] H. Schmidt, J. Non-Cryst. Solids 178 (1994) 302.
- [11] Y. Sorek, R. Reisfeld, A.M. Weiss, Chem. Phys. Lett. 244 (1995) 371.
- [12] E.T. Knobbe, B. Dunn, P.D. Fuqua, F. Nishida, Appl. Opt. 29 (1994) 2729.
- [13] S.J.L. Ribeiro, Y. Messaddeq, R.R. Gonçalves, M. Ferrari, M. Montagna, M.A. Aegerter, Appl. Phys. Lett. 77 (2000) 3502.
- [14] Wenxiu Que, Y. Zhou, Y.L. Lam, J. Zhou, Y.C. Chan, C.H. Kam, J. Appl. Phys. 89 (2001) 3058.
- [15] S.W. Kim, S. Fujita, Appl. Phys. Lett. 81 (2002) 5036.
- [16] X.W. Sun, H.S. Kwok, J. Appl. Phys. 86 (1999) 408.
- [17] S.N.B. Bhaktha, F. Beclin, M. Bouazaoui, B. Capoen, A. Chiasera, M. Ferrari, C. Kinowski, G.C. Righini, O. Robbe, S. Turrell, Appl. Phys. Lett. 93 (2008) 211904.
- [18] A. Peled, A. Chiasera, M. Nathan, M. Ferrari, S. Ruschin, Appl. Phys. Lett. 92 (2008) 221104.
- [19] G. Nunzi Conti, N. Peyghambarian, M. Ferrari, M. Montagna, G.C. Righini, M. Brenni, M.A. Forestiere, S. Pelli, G. Ricci, Philos. Mag. B 82 (2002) 721.
- [20] K.S. Chiang, IEEE/OSA J. Lightwave Technol. LT-3 (1985) 385.
- [21] Wang Zhi-Jun, Song Li-Jun, Li Shou-Chun, Lu You-Ming, Tian Yun-Xia, Liu Jia-Yi, Chinese Phys. 15 (2006) 2710.
- [22] H. Zhang, G. Chen, G. Yang, J. Zhang, X. Lu, J. Mater. Sci.: Mater. Electron. 18 (2007) 381.
- [23] P.T. Huy, N.D. Chien, M. Ferrari, Dojin Kim, in: Proceedings of the ICPE 2006 International Conference on Engineering Physics, Hanoi, 9th October 2006, p. 6.
- [24] W. Gao, Z.W. Li, J. Alloy. Compd. 449 (2008) 202.